Nucleolar KKE/D repeat proteins Nop56p and Nop58p interact with Nop1p and are required for ribosome biogenesis

MOLECULAR AND CELLULAR BIOLOGY, Dec. 1997, p. 7088–7098 Vol. 17, No. 12
0270-7306/97/$04.00+0

Nucleolar KKE/D Repeat Proteins Nop56p and Nop58p Interact with Nop1p and Are Required for Ribosome Biogenesis

THIERRY GAUTIER,[1] THIERRY BERGÈS,[2] DAVID TOLLERVEY,[3] AND ED HURT[4]*

Laboratoire DyOGen, Institut Albert Bonniot, Université Grenoble I, Domaine de la Merci, F-38706 La Tronche Cedex,[1] and Institut Biologie Moléculaire et d'Ingénierie Génétique, Université de Poitiers, F-86022 Poitiers Cedex,[2] France; Institute of Cell and Molecular Biology, University of Edinburgh, Edinburgh EH9 3JR, United Kingdom[3]; and Biochemie-Zentrum Heidelberg, Universität Heidelberg, D-69120 Heidelberg, Germany[4]

Received 16 June 1997/Returned for modification 14 July 1997/Accepted 19 September 1997

Different point mutations in the nucleolar protein fibrillarin (Nop1p in *Saccharomyces cerevisiae*) can inhibit different steps in ribosome synthesis. A screen for mutations that are synthetically lethal (sl) with the *nop1-5* allele, which inhibits pre-rRNA processing, identified *NOP56*. An independent sl mutation screen with *nop1-3*, which inhibits pre-rRNA methylation, identified a mutation in *NOP58*. Strikingly, Nop56p and Nop58p are highly homologous (45% identity). Both proteins were found to be essential and localized to the nucleolus. A temperature-sensitive lethal mutant allele, *nop56-2*, inhibited many steps in pre-rRNA processing, particularly on the pathway of 25S/5.8S rRNA synthesis, and led to defects in 60S subunit assembly. Epitope-tagged constructs show that both Nop56p and Nop58p are associated with Nop1p in complexes, Nop56p and Nop1p exhibiting a stoichiometric association. These physical interactions presumably underlie the observed sl phenotypes. Well-conserved homologs are present in a range of organisms, including humans (52% identity between human hNop56p and yeast Nop56p), suggesting that these complexes have been conserved in evolution.

Most steps of ribosome biogenesis occur in the nucleolus, a specialized subnuclear structure (for reviews, see references 14, 34, 39, 45, and 53). In eukaryotes including *Saccharomyces cerevisiae* and humans, a large precursor rRNA transcript (pre-rRNA) is processed into the mature 18S, 5.8S, and 25S/28S rRNAs. During transcription and processing, these rRNAs associate with approximately 80 ribosomal proteins and with the 5S rRNA. In addition, the mature rRNA regions of the pre-rRNA undergo extensive covalent nucleotide modification, mainly base modification of uridine to pseudouridine and methylation of the ribose 2′-hydroxyl (2′-O methylation) (reviewed in reference 27). The large number of concerted reactions occurring during rRNA processing and ribosome assembly has made it difficult to analyze single steps in ribosome synthesis. Over recent years, the analysis of yeast mutants defective in ribosome biogenesis has proved to be a powerful approach (reviewed in reference 51), particularly when combined with in vitro analyses using purified components (8, 26, 30). Despite this progress, our understanding of the detailed mechanisms of eukaryotic rRNA processing remains poor.

The small nucleolar RNAs (snoRNAs) play important roles in the covalent processing of the pre-rRNAs (reviewed in references 2, 28, and 48). With the exception of RNase MRP, which is an endonuclease structurally related to RNase P, the very large numbers of snoRNAs present in eukaryotes can be divided into two groups based on conserved sequence and structural features (3, 12; reviewed in reference 48). Most of the box C+D snoRNAs direct the site-specific 2′-O methylation of the pre-rRNA (19), while most of the box H+ACA snoRNAs select the sites of pseudouridine formation (6, 11, 33). In addition, a few members of each group of snoRNAs do not appear to select sites of pre-rRNA modification but are required for normal pre-rRNA processing. In yeast, these include the box C+D snoRNAs U3 (4, 15) and U14 (25) and the box H+ACA snoRNAs snR10 (47) and snR30 (32); genetic depletion of any of these snoRNAs inhibits the early pre-rRNA cleavages on the pathway of 18S rRNA synthesis.

Nop1p is the yeast homolog of the vertebrate nucleolar protein fibrillarin; the two proteins are 70% identical, and the human protein is able to function in yeast, indicating an extremely high degree of evolutionary conservation (1, 16). Initial reports concluded that Nop1p was associated with all yeast snoRNAs, but more recent analyses indicated that the association with H+ACA snoRNAs is more labile than association with the box C+D snoRNAs, and human fibrillarin does not appear to be associated with the H+ACA snoRNAs (reference 12 and references therein). From a bank of temperature-sensitive (ts) lethal mutations in *NOP1*, alleles with quite distinct effects on ribosome synthesis were isolated (49). The *nop1-2* and *nop1-5* alleles inhibited many pre-rRNA processing steps. In the *nop1-5* strain, synthesis of the 60S subunit rRNAs, 5.8S and 25S, was more strongly inhibited than synthesis of the 18S rRNA. In contrast, the *nop1-3* mutation had little effect on processing but blocked 2′-O methylation at the nonpermissive temperature (49). Whether the lethality was a consequence of the synthesis of ribosomes lacking methylation or was due to some effect of *nop1-3* on ribosome assembly could not be determined. All tested methylation guide snoRNAs are dispensable for viability, but it is certainly possible that the loss of all methylation would be lethal. Other alleles, *nop1-4* and *nop1-7*, interfered with the assembly of ribosomal subunits, with 60S assembly being most clearly affected. The processing defects associated with the *nop1-5* mutation and the assembly defects associated with *nop1-4* and *nop1-7* mutations do not

* Corresponding author. Mailing address: Biochemie-Zentrum Heidelberg, Universität Heidelberg, Im Neuenheimer Feld 328, D-69120 Heidelberg, Germany. Phone: 49 6221 544 173. Fax: 49 6221 544 369. E-mail: cg5@ix.urz.uni-heidelberg.de.

TABLE 1. Yeast strains

Strain	Genotype	Reference
RS453	*MAT***a**/α *ade2/ade2 his3/his3 trp1/trp1 leu2/leu2 ura3/ura3*	
sl258	*MAT***a** *ade2 ade3 leu2 ura3 HIS3/nop1-5 can1 nop56sl* pCH1122-URA3-ADE3-NOP1	4a
Δ258-42D	*MAT***a**/α *ade2/ade2 his3/HIS3::nop56/NOP56 trp1/trp1 leu2/leu2 ura3/ura3*	4a
shuffle56	*MAT***a** *ade2 HIS3::nop56 trp1 leu2 ura3* pRS316-NOP56	This study
shuffle58	*MAT***a** *ade2 HIS3::nop58 trp1 leu2 ura3* pRS316-NOP58	This study
ProtA-NOP56	*MAT***a** *ade2 ade3 leu2 ura3 nop56::HIS3* pRS315-ProtA-NOP56	This study
ProtA-NOP56ΔKKE	*MAT***a** *ade2 ade3 leu2 ura3 nop56::HIS3* pRS315-ProtA-NOP56ΔKKE	This study
Myc-NOP56ΔKKE	*MAT***a** *ade2 ade3 leu2 ura3 nop56::HIS3* pRS314-Myc-NOP56ΔKKE	This study
nop56-1 mutant	*MAT***a** *ade2 HIS3::nop56 trp1 leu2 ura3* pRS315-NOP56-1	This study
nop56-2 mutant	*MAT***a** *ade2 HIS3::nop56 trp1 leu2 ura3* pRS315-NOP56-2	This study
ProtA-NOP58	*MAT***a** *ade2 ade3 leu2 ura3 can1 nop58::HIS3* pRS315-ProtA-NOP58	This study
ProtA-NOP58ΔKKE	*MAT***a** *ade2 ade3 leu2 ura3 nop58::HIS3* pRS315-ProtA-NOP58ΔKKE	This study
Myc-NOP58ΔKKE	*MAT***a** *ade2 ade3 leu2 ura3 nop58::HIS3* pRS314-Myc-NOP58ΔKKE	This study
ΔKKE	*MAT***a** *ade2 ade3 leu2 ura3 nop58::HIS3 nop56::HIS3* pRS314-Myc-NOP56ΔKKE pRS315-ProtA-NOP58ΔKKE	This study

resemble those of any characterized yeast snoRNA, suggesting that Nop1p may have functions, and be present in complexes, which are independent of the snoRNAs.

Genetic analyses have identified proteins that interact with Nop1p: Sof1p (17) as an extragenic suppressor of the ts lethality of strains having *NOP1* deleted and expressing human fibrillarin and Nop77p (5) as synthetic lethal (sl) with the *nop1-5* mutation. Both Sof1p, which is a U3-small nucleolar ribonucleoprotein particle protein, and Nop77p, which is not detectably associated with snoRNAs, are physically associated with Nop1p, but only in substoichiometric amounts.

To identify additional components which interact with Nop1p, we screened for sl mutants by using the *nop1-5* and *nop1-3* alleles (5). These screens identified the novel genes *NOP56* (for nucleolar protein of 56 kDa) and *NOP58*, respectively. We found that both encode essential nucleolar proteins, which are significantly homologous to each other. Moreover, the Nop56p protein is recovered in stoichiometric complexes with Nop1p.

MATERIALS AND METHODS

Strains, plasmids, and media. Preparation of yeast media, growth of yeast, and its genetic manipulation were performed as previously described (5, 40). Strains used in this study are described in Table 1. Strains synthetically lethal with *nop1.5*, sl258 and sl326, were described by Bergès et al. (5). Plasmids used in this study were the following: pUN100 (9); pRS3XX series (41), which are ARS1/CEN4 plasmids with the *LEU2*, *URA3*, and *TRP1* markers; pCH1122 (20), which contains the *ADE3* and *URA3* marker, used for the red-white colony sectoring assay; pBluescript (Stratagene); pRS315-NOP56 and pRS316-NOP56, containing the genomic *NOP56* gene inserted as a 4.3-kb *Spe*I-*Sac*I fragment; pRS315-ProtA-NOP56, containing the *ProtA::NOP56* fusion gene in which two immunoglobulin G (IgG) binding domains derived from *Staphylococcus aureus* protein A (ProtA) were fused in frame to the N-terminal end of the *NOP56* gene; pRS315-ProtA-NOP56ΔKKE, corresponding to a construct in which a stop codon was generated within the *NOP56* gene by mutagenesis at the 5′ site corresponding to the first KKE repeat motif; pRS314-Myc-NOP56ΔKKE, constructed by cloning NOP56ΔKKE from pRS315-ProtA-NOP56ΔKKE into pRS314-Myc as a *Pst*I-*Xho*I fragment; pRS315-NOP58, containing the *NOP58* gene inserted as a 2.4-kb PCR fragment from genomic DNA; pRS315-ProtA-NOP58, containing the *ProtA::NOP58* fusion gene in which two IgG binding domains derived from *S. aureus* ProtA were fused in frame to the 5′ end of the *NOP58* gene. For pRS315-ProtA-NOP58ΔKKE, a *Bam*HI site was inserted before the first KKE/D motif into pRS315-ProtA-NOP58. The plasmid was then cut with *Bam*HI, filled in, and religated, which caused a frameshift and generation of a stop codon before the KKE/D motif. pRS314-Myc-NOP58ΔKKE was constructed by cloning NOP58ΔKKE from pRS315-ProtA-NOP58ΔKKE into pRS314-Myc as a *Pst*I-*Xho*I fragment.

Cloning, sequencing, and disruption of *NOP56*. *NOP56* was isolated by complementation of one of the remaining *nop1-5* sl mutants, called sl258, described by Bergès et al. (5). For this cloning, sl258 was transformed with a yeast genomic library present in an ARS/CEN-LEU2 plasmid. The total number of transformants was ~4,500, from which 3 exhibited a red-white sectoring phenotype after 6 days of incubation on yeast extract-peptone-dextrose. Restriction analysis of the recovered plasmids indicated that two were carrying a copy of *NOP1* while the third one contained a 13-kb insert not related to *NOP1*, *NOP77*, or *SOF1*. The complementing region was restricted to a 2.1-kb genomic fragment inserted into plasmid pRS315, and the DNA was sequenced. During the time course of this study, *NOP56* was also sequenced within the yeast genome sequencing project as a potential open reading frame (ORF) on chromosome XII (accession no. U14913). The gene was disrupted by first subcloning a genomic *Eco*RV fragment containing the central part of *NOP56* into pBluescript. From this fragment, a 0.5-kb *Nco*I fragment (corresponding to amino acids 259 to 430) was replaced by a 1.1-kb-long *Bam*HI fragment containing the *HIS3* gene. The *nop56::HIS3* construct was excised with *Eco*RV and used to transform a diploid RS453 strain. Correct integration of the *nop56::HIS3* construct at the homologous locus was confirmed by Southern blot analysis of HIS^+ transformants. Two independent correct integrants were sporulated, and tetrads were dissected.

Cloning, disruption, and screening of *NOP58*. *NOP58* was cloned by PCR from genomic DNA as a *Spe*I-*Xho*I fragment and inserted into plasmid pRS315. The internal *Hin*dIII and *Sty*I sites were used to exchange the central part of the coding sequence (corresponding to amino acids 17 to 467) with the *HIS3* gene. The disrupted *nop58::HIS3* gene was recovered as a *Spe*I-*Xho*I fragment and transformed into the diploid RS453 strain. Analysis of the *nop58::HIS3* disruption was performed as described for *nop56::HIS3* disruption.

The strain used for the sl screen with the *nop1-3* allele was constructed essentially as described for the *nop1-5* allele (5). The strain was UV mutagenized, and nonsectoring clones were scored at 28°C, out of 25,000 to 30,000 surviving colonies (90% killing rate). A total of 12 correct sl colonies (i.e., sectoring when transformed with the wild-type *NOP1* allele and nonsectoring when transformed with the *nop1-3* allele) were kept for further studies. These 12 candidates were transformed with a series of genes coding for known nucleolar proteins (Sof1p, Nop77p/Nop4p, Nop56p, and Nop58p). One of the mutants, sl28, clearly regained sectoring when transformed with *NOP58*, while three could be complemented with *NOP77*, and none could be complemented with *SOF1* or *NOP56*.

Construction of ProtA and Myc fusion proteins. The ProtA tag used in this work consisted of two IgG binding domains under control of the *NOP1* promoter fused in frame to the 5′ end of the *NOP56* and *NOP58* genes (13). The full-length *ProtA-NOP56* fusion gene was obtained by the ligation of a *Bam*HI-*Pst*I fragment containing the *NOP1* promoter plus the IgG binding domain to a *Pst*I-*Hin*dIII PCR fragment corresponding to the *NOP56* ORF plus 3′ noncoding sequences and subcloning into plasmid pRS315 previously digested with *Bam*HI and *Hin*dIII. The full-length *ProtA-NOP58* fusion gene was obtained by subcloning a *Pst*I-*Xho*I PCR fragment of *NOP58* into pRS315-ProtA, followed by insertion of the internal 0.15-kb *Pst*I of *NOP58* into the previously generated unique *Pst*I site, and checked for correct orientation. To generate the *ProtA-NOP56ΔKKE* fusion gene, two primers were designed to change the GATGAAGAAAAG DNA sequence of *NOP56* into GATGAATAAAAG, thereby generating a premature stop codon within *NOP56* at a position which corresponds to the last amino acid before the first KKE motif (amino acid 464). pRS315-ProtA-NOP58ΔKKE was constructed by inserting a *Bam*HI site at amino acid position 450. The *Bam*HI site was then cut open, filled in, and religated, thereby generating a frameshift mutation (from 451-KKEKKEKKRKRDDD-464 to 451-KERKERKEEKERR-stop-463). *NOP1* was also tagged with ProtA at its N-terminal end. For Myc tagging, a DNA fragment containing three Myc epitopes in tandem (S. Kron, Whitehead Institute, Cambridge, Mass.) was cloned under the control of the *NOP1* promoter and inserted into plasmid pRS314. The full-length Myc-*NOP56ΔKKE* fusion gene was generated by subcloning appropriate *Pst*I-*Hin*dIII and *Hin*dIII-*Eco*RV fragments into plasmid pRS314-Myc at the *Pst*I-*Eco*RV sites. The Myc-*NOP58ΔKKE* gene was generated by subcloning the *Pst*I-*Pst*I and *Pst*I-*Xho*I fragment into pRS314-Myc at the *Pst*I-*Xho*I sites.

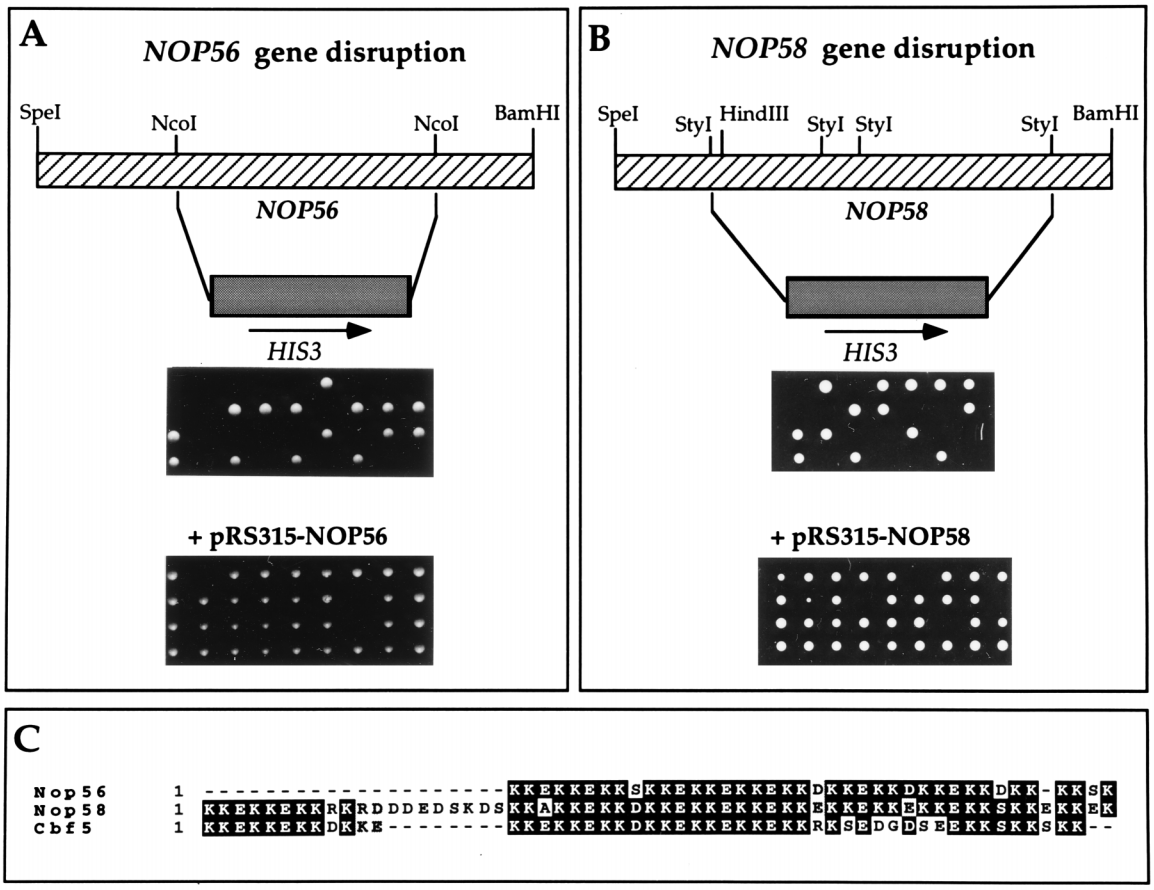

FIG. 1. (A and B) Disruption of *NOP56* (A) and *NOP58* (B). Tetrad analysis of the disrupted strains shows that both genes are essential for cell viability and can be complemented by the CEN/ARS plasmid harboring the wild-type allele. (C) Alignment of the KKE/D repeated motif at the COOH termini of each protein. Overall identity reaches 85%. (D) Alignment of Nop56p and Nop58p with their putative homologs in humans and *C. elegans*. (E) Alignment of Nop56p, Nop58p, and Prp31p showing blocks of conserved amino acids.

Protein purification of ProtA fusion proteins by IgG-Sepharose chromatography from whole-cell extracts under nondenaturing conditions was done according to the method of Siniossoglou et al. (44). Cells expressing the fusion proteins were converted to spheroplasts and lysed in 2% Triton X-100–150 mM KCl–20 mM Tris (pH 8.0)–5 mM $MgCl_2$, supplemented with a cocktail of protease inhibitors. Protein extracts were analyzed by sodium dodecyl sulfate (SDS)–10% polyacrylamide gel electrophoresis (PAGE) and Western blotting.

The strain disrupted for both *NOP56* and *NOP58* was constructed by crossing individual strains of opposite mating type expressing pRS315-ProtA-Nop56ΔKKE and pRS314-Myc-Nop58ΔKKE, respectively. The latter expressed also pRS316-ProtA-Nop56p. After tetrad dissection and analysis of the genotype, the haploid *nop56*/*nop58* null strain containing pRS315-ProtA-Nop56ΔKKE and pRS314-Myc-Nop58ΔKKE was shown to survive on 5-fluoroorotic acid (5-FOA)-containing plates. The subsequent strain (Table 1) was used to assess the existence of a Nop56p-Nop58p-Nop1p complex.

Indirect immunofluorescence. Immunolocalization of the ProtA-Nop56p/Nop58p fusion proteins was done as previously described (13, 44). When the double immunofluorescence assay was performed, monoclonal antibody A66 against Nop1p was used (kindly provided by J. Aris, University of Florida).

Generation of thermosensitive *nop56* mutants. To generate mutations within *NOP56*, a PCR-mediated mutagenesis approach was used (24). The *NOP56* gene was subcloned as a 2.1-kb *Spe*I-*Bam*HI fragment into plasmid pRS315, in which the *Xba*I polylinker site was destroyed. This rendered the two *Xba*I sites within *NOP56* unique in this plasmid. The DNA between these two *Xba*I sites was mutagenized by PCR. A bank of mutated *nop56* was obtained from 600 *Escherichia coli* transformants. Six microliters of the DNA was used to transform a *NOP56* shuffle strain (Table 1). A total of 800 LEU^+ transformants were transferred on SDC (−Leu) plates at 23°C before shuffling out the pRS316-NOP56 plasmid on 5-FOA at 23°C. The 400 survivors were then assessed for a thermosensitive phenotype by incubation at 23 and 37°C for 3 days. From two transformants exhibiting a growth defect at 37°C, the corresponding plasmids were recovered and shown to cause a ts phenotype when reintroduced into a *nop56::HIS3* strain. A 0.5-kb *Nco*I fragment which includes the *nop56-2* mutation was further shown to be sufficient to cause the thermosensitive phenotype (12a).

RNA extraction, hybridization, and pulse-chase of rRNA. RNA extraction, gel electrophoresis, and hybridization were performed as described elsewhere (47). For pulse-chase labeling, *nop56-2* and *NOP56* cells were grown to an optical density at 600 nm (OD_{600}) of 0.4 at 23°C, diluted to an OD_{600} of 0.1, shifted to the restrictive temperature, and further incubated for 6 h before labeling. For the pulse, 100 μCi of [^{3}H]uracil was added to 4 ml of cells at an OD_{600} of 0.3 and incubated for 2 min; for the chase, a large excess of unlabeled uracil (1/20 volume at 0.24 μg ml^{-1}) was added. One-milliliter aliquots were taken at intervals, immediately pelleted by centrifugation at 14,000 rpm for 20 s, and frozen in −80°C cold ethanol. RNA extraction was performed in parallel for all samples as described elsewhere (37). For steady-state level analysis, RNA was extracted from a total of 40 OD_{600} units of cells at each time point and 4 μg of RNA of each sample was loaded on the gel before Northern blot hybridization with the indicated probes.

Miscellaneous. To clone the complete ORF of human *hNOP56*, a HeLa cell cDNA library in *E. coli* was probed by colony hybridization with the *EST* sequence homologous to Nop56p (accession no. T08589), which was obtained from the American Type Culture Collection. Two positive cDNA clones were sequenced and shown to contain the entire ORF of human *NOP56*. All sequencing work for *hNOP56* and *NOP56* was performed by primer walking by the dideoxy sequencing method (38), and comparisons were done with the FASTA algorithms from the GCG software package. DNA manipulations, including restriction analysis, fill-in reactions with Klenow and T4 DNA polymerases, ligations, PCR, and Southern blots, were done essentially according to the methods described by Maniatis et al. (27a). For Western blot analysis, anti-ProtA antibodies coupled to horseradish peroxidase were diluted 1:1,000 and incubated for 30 min at room temperature. Anti-Nop1p antibodies (A66) were diluted 1:100 for immunofluorescence and incubated for 30 min at room temperature or diluted 1:400 for Western blot analysis and incubated for 2 h at room temperature.

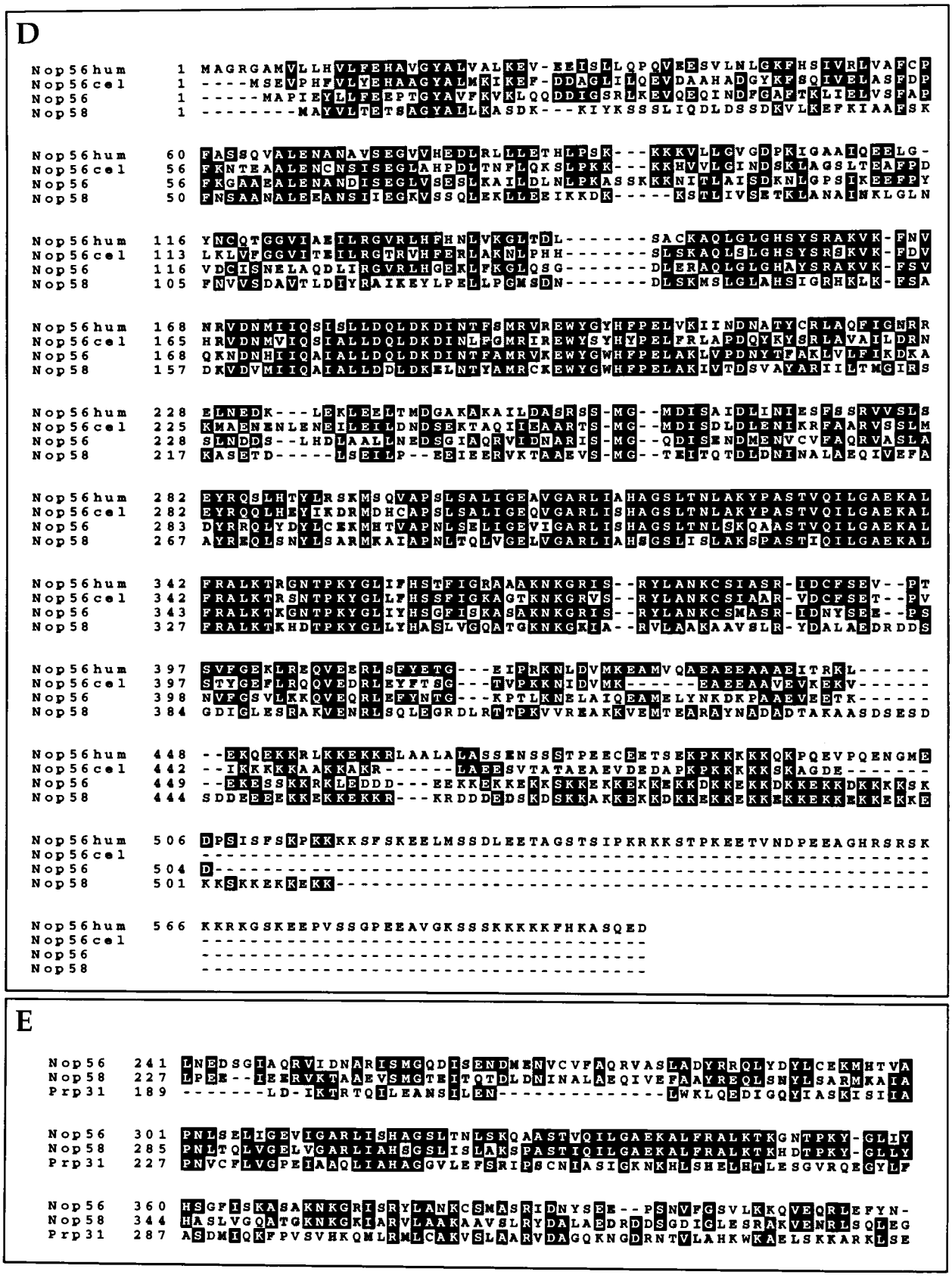

FIG. 1—*Continued.*

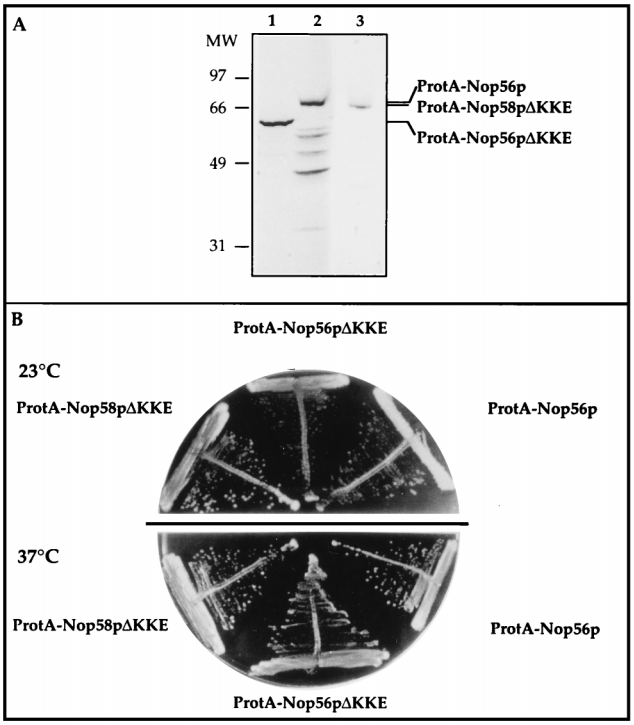

FIG. 2. (A) Western blot of proteins from strains expressing tagged versions of Nop56p and Nop58p detected with anti-ProtA antibodies (1:1,000). Extracts are from strains expressing ProtA-Nop56pΔKKE (lane 1), ProtA-Nop56p (lane 2), and ProtA-Nop58ΔKKE (lane 3). MW, molecular weight in thousands. (B) Growth comparison of strains carrying chromosomal gene disruptions complemented by expression of the tagged proteins. The strains complemented by the tagged proteins show no growth defects at 37 or 23°C compared to the strain expressing full-length ProtA-Nop56p. The tagged constructs are functional, and the KKE/D motifs are not required for cell viability.

Anti-Myc antibodies from mouse ascites (9E10) were diluted to 1:100 and incubated for 2 h at room temperature.

Nucleotide sequence accession number. The DNA sequence of the ORF of human *hNOP56* is in the EMBL nucleotide data library under accession no. Y12065.

RESULTS

Synthetic lethality with *nop1* mutants identifies two novel genes, *NOP56* and *NOP58*. In a search for novel components of the ribosome synthesis machinery, we undertook screens for mutations which are sl with ts mutations in *NOP1*. Using the *nop1-5* ts allele as the target, we isolated 14 sl mutant strains (5). Twelve of these strains were complemented by the *NOP77* gene (5). *NOP56*, for nucleolar protein of 56.8 kDa, was identified as a clone which complemented the sl mutation in strain sl258 (Table 1; see also Materials and Methods). *NOP56* is located on chromosome XII and encodes a polypeptide of 504 amino acids with a predicted molecular mass of 56.8 kDa. A search of the yeast genomic database identified another ORF (accession no. X90565) (36), which is located on chromosome XV and encodes a polypeptide of 511 amino acids, that we designated *NOP58*. Nop56p and Nop58p are highly homologous (45% identical and 63% similar) over their entire sequences (Fig. 1D). During this work, *NOP56* was independently identified as a high-copy-number suppressor, named *SIK1* (accession no. U20237), of the growth-inhibitory activity of GAL4-Iκβ and LEXA-Iκβ fusion proteins (31).

The C-terminal regions of both proteins contain a repeated sequence with the motif KKE/D (Fig. 1C). This motif is also present in the yeast nucleolar protein Cbf5p (18, 29), and a similar motif (KKX) is found in Dbp3p (54). Nop56p contains 11 repeats, while Nop58p and Cbf5p both have 13 (Fig. 1C) and Dbp3 has 10 (KKX) repeats (54). The overall identity among the three sequences reaches 85% over the KKE/D motifs. Furthermore, Nop56p and Nop58p share homology to several *EST* sequences derived from human, rice, and *Caenorhabditis elegans* cDNAs (Fig. 1D). Using the human *EST* sequence as probe, we cloned the corresponding cDNA from a HeLa cell cDNA library and sequenced the entire ORF of a putative human homolog of Nop56p, called hNop56p (accession no. Y12065). The human protein of 611 amino acids is 52% identical and 68% similar to Nop56p, whereas the homology of hNop56p to yeast Nop58p is lower (41% identity and 57% similarity). Curiously, the human hNop56p lacks the C-terminal KKE/D motifs present in the yeast proteins (Fig. 1D) and cannot complement a *nop56* null strain (data not shown). Finally, both Nop56p and Nop58p show some homology (21% identity and 45% similarity) to the yeast pre-mRNA splicing factor Prp31p (55). Sequence alignment among these three proteins is shown in Fig. 1E.

Nop56p and Nop58p are essential nucleolar proteins. In order to analyze its in vivo function, the *NOP56* gene was disrupted by replacing an internal *Nco*I fragment with the *HIS3* gene, deleting 40% of the coding sequence (Fig. 1A). The correct integration of the disrupted allele was confirmed by Southern blot analysis. Two independent heterozygous diploids were sporulated; in each case, tetrad analysis showed 2:2 segregation for cell viability. All viable spores were His^-. When the heterozygous diploid was transformed with plasmid pRS315-NOP56 and then sporulated, tetrads yielded mostly

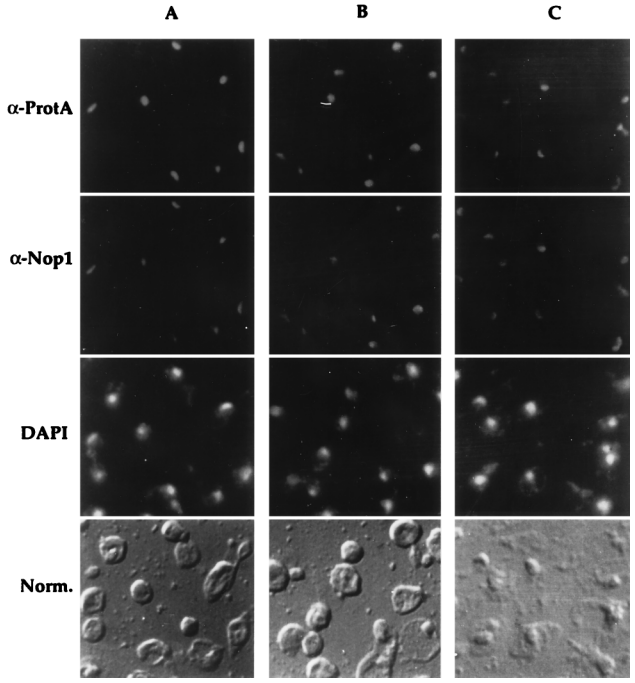

FIG. 3. Indirect immunofluorescence assay of ProtA-tagged proteins. (A) Localization of ProtA-Nop56p. (B) Localization of ProtA-Nop56pΔKKE. (C) Localization of ProtA-Nop58ΔKKE. In all cases, the proteins localize in the nucleolus, exhibiting the characteristic crescent-like shape, and colocalize with Nop1p, used as a marker for the nucleolus. DNA staining with Hoechst 33258 dye is shown together with a Nomarski (Norm.) view of each field. The lack of the KKE/D motif does not perturb the nucleolar localization of the proteins. DAPI, 4′,6-diamidino-2-phenylindole.

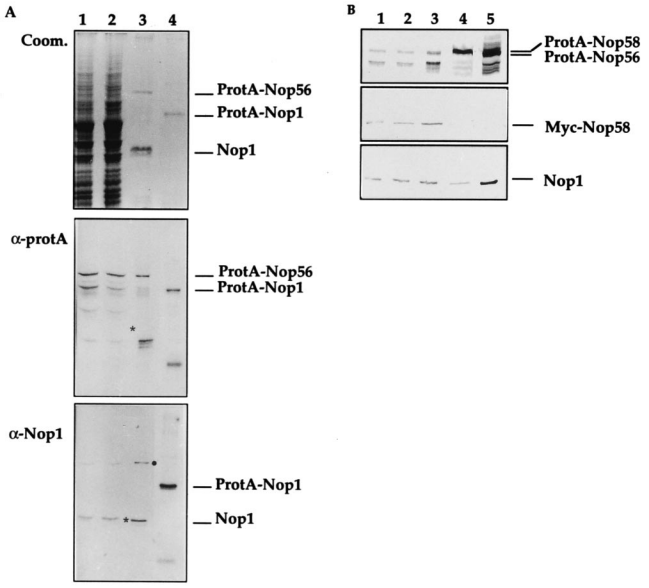

FIG. 4. Affinity purification of the Nop56p complex. (A) After affinity purification, a sample of the homogenate (lane 1), the supernatant (lane 2), and 400 times the equivalent of the eluate (lane 3) were analyzed by SDS–10% PAGE. Coomassie blue staining reveals the presence of two proteins in the eluate migrating at the position of ProtA-Nop56pΔKKE and Nop1p. By comparison, the eluate obtained after affinity purification of ProtA-Nop1p (lane 4) does not show associated proteins. Anti-ProtA antibodies specifically detect the ProtA-Nop56p band in each fraction. The second blot was detected with mouse monoclonal anti-Nop1 antibodies (1:400). After Ponceau Red staining, the position of the visible lower band in the eluate was marked prior to incubation with the antibodies and is indicated by an asterisk. It is evident that this band corresponds to Nop1p and not to degradation products of ProtA-Nop56ΔKKE. The dot indicates the position of ProtA-Nop56ΔKKE, which cross-reacts with the antibodies used to detect Nop1p because of the ProtA tag. (B) Affinity purification of the Nop56p-Nop58p-Nop1p complex. Affinity-purified ProtA-Nop56p copurifies with Myc-Nop58p and Nop1 (lane 3). Lanes 1 and 2 correspond to homogenate and supernatant of the cell lysis procedure, respectively. Lanes 4 and 5 correspond to eluate from precipitations with ProtA-Nop58ΔKKE and ProtA-Nop56ΔKKE, respectively. Blots were probed, from top to bottom, with anti-ProtA antibodies, anti-Myc antibodies, and anti-Nop1p antibodies, as for panel A.

three or four viable progeny. This indicates that a short deletion of the coding sequence was sufficient to abolish the function of the protein which is essential for cell viability.

The *NOP58* gene was recovered by genomic PCR and shown to be correct by sequencing; the clone used for further analysis was shown to fully complement a chromosomal deletion of *NOP58*. A mutation isolated in the sl screen with the *nop1-3* allele was found to be complemented by the cloned *NOP58* gene (see Materials and Methods). The *NOP58* gene was disrupted by using an approach similar to that described for *NOP56* (see Materials and Methods); subsequent analysis showed that Nop58p is also required for cell viability (Fig. 1B). Despite their homology, neither Nop56p nor Nop58p acted as a multicopy suppressor of the disruption of the other, nor was cross-complementation of the sl strains observed.

To determine their intracellular localization, tagged fusion proteins were constructed by the insertion of two IgG binding domains from the *S. aureus* ProtA at the N termini of Nop56p and Nop58p (see Materials and Methods). The plasmids were introduced into the respective deletion strains by plasmid exchange (see Materials and Methods). Expression of the ProtA-Nop56p fusion protein was assessed by Western blotting; Fig. 2A, lane 2, shows that the fusion protein migrated at the expected position in the gel (70 kDa). Expression of ProtA-Nop56p fully complemented a *nop56* null strain for growth at 23 and 37°C (Fig. 2B). Indirect immunofluorescence assay performed on this strain revealed a cap-like nuclear staining pattern for the fusion protein, which is characteristic of nucleolar localization. When immunolocalization was performed together with an anti-Nop1 antibody, both signals colocalized in the nucleoli (Fig. 3A). The ProtA-Nop58p fusion was similarly shown to be functional (Fig. 2B and data not shown) and to be localized in the nucleolus by immunofluorescence (Fig. 3C and data not shown).

The KKE/D motif is not required for the function of Nop56p or Nop58p. To assess the function of the repeated KKE/D motifs at their C termini, the last codons before the first repeated motif of Nop56p and Nop58p were exchanged for stop codons in the tagged protein constructs. The resulting truncated proteins (ProtA-Nop56ΔKKE and ProtA-Nop58ΔKKE) were transformed into the corresponding deletion strains, which also carried the wild-type alleles on *URA3* plasmid vectors. Correct expression of the fusion proteins was confirmed by Western blotting (Fig. 2A, lanes 1 and 3). Growth on medium containing 5-FOA, which selects for loss of the wild-type, *URA3*-containing plasmids, indicated that the truncation did not impair the cell viability; no difference in growth was observed when the cells were grown on yeast extract-peptone-dextrose plates at 23 or 37°C (Fig. 2B). As expected from the complementation result, indirect immunofluorescence assay performed on cells expressing ProtA-Nop56ΔKKE (Fig. 3B) or ProtA-Nop58ΔKKE (Fig. 3C) showed correct targeting of the fusion proteins to the nucleolus. Positions of the nucleoli are indicated by the anti-Nop1 staining, which colocalizes with the anti-ProtA staining.

Nop56p exists in a stable complex with Nop1p. The ProtA-tagged fusion proteins were used to search for physical interactions with other components. When affinity purification under nondenaturing conditions was performed with strains expressing the full-length ProtA-Nop56p fusion protein, degradation occurred during the elution and concentration steps.

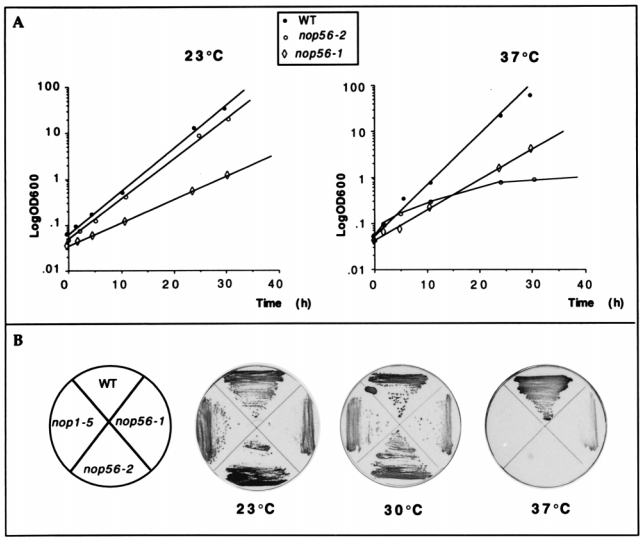

FIG. 5. Growth of the ts *nop56* mutants. (A) Growth of the *nop56-1* strain is slowed at 23 and 37°C. Growth of the *nop56-2* strain is similar to that of the *NOP56* control at 23°C but slows 6 to 8 h after transfer to 37°C, ceasing after 20 h at 37°C. (B) Appearance of the colonies on plates at different temperatures. Compared to the *NOP56* strain, the *nop56-1* strain displays slow growth at all temperatures. The *nop1-5* and *nop56-2* strains form colonies similar in size to those of the *NOP56* strain at 23 or 30°C but do not grow at 37°C. WT, wild type.

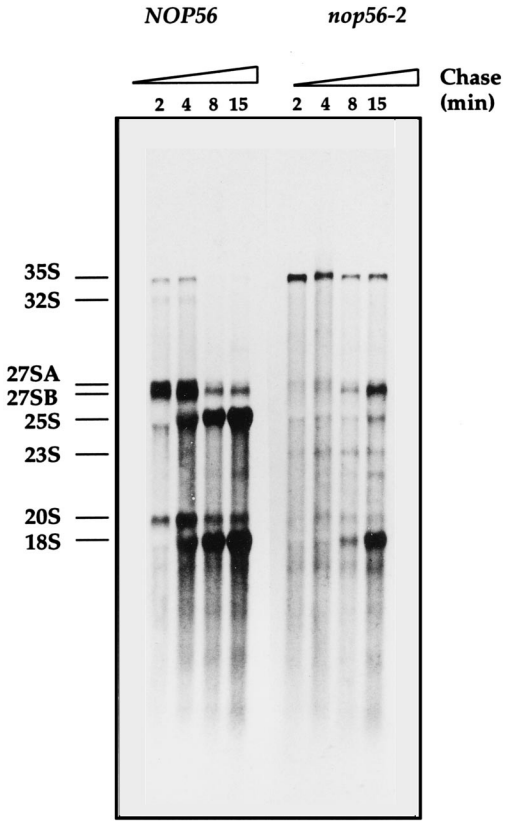

FIG. 6. Analysis of rRNA maturation by pulse-chase labeling. Following transfer to 37°C for 6 h, cells were pulse-labeled with [^{3}H]uracil for 1 min and then chased with a large excess of unlabeled uracil for the times indicated. Total RNA was recovered, separated by gel electrophoresis, and visualized by fluorography.

Even in the presence of a cocktail of protease inhibitors, no full-length fusion protein could be detected in the eluate (data not shown). The ProtA-Nop56ΔKKE fusion protein was substantially more stable than full-length ProtA-Nop56p and was therefore used for the purification shown in Fig. 4A. Coomassie blue staining of the eluate revealed two major bands migrating at about 60 and 36 to 38 kDa and present in approximately stoichiometric amounts (Fig. 4A, lane 3). The upper band was detected by anti-ProtA antibodies and was identified as ProtA-Nop56ΔKKE. The lower band was detected by both mouse monoclonal anti-Nop1p (Fig. 4A) and rabbit polyclonal anti-Nop1p antibodies (data not shown). On each filter, the position of the lower band visible after staining with Ponceau Red was marked (indicated by asterisks on Fig. 4A). The position of this species corresponds to the band detected by the mouse monoclonal anti-Nop1 antibodies (Fig. 4A, panel α-Nop1) but does not correspond to any major degradation products from ProtA-Nop56pΔKKE (Fig. 4A, panel α-ProtA). Nop1p was also copurified from cell extracts expressing ProtA-Nop56pΔKKE (data not shown), even though the full-length ProtA-Nop56p was degraded to smaller breakdown products. This suggests that proteolysis of ProtA-Nop56p occurred probably only during the steps required for elution but not in the cell.

As a control for affinity purification, a nonfunctional ProtA-Nop56p construct was used in parallel experiments; this showed no copurification of Nop1p in the eluate (data not shown). The mutation corresponded to a deletion of 10 amino acids between positions 378 and 388 obtained by deletion of an internal *Xba*I-*Xba*I fragment.

In a parallel experiment, a ProtA-Nop1p fusion protein was used for immunoprecipitation. No copurifying species were clearly detected by Coomassie blue staining (Fig. 4A, lane 4). Nop1p is associated with a very large number of different components of the ribosome synthesis machinery, probably including more than 50 different small nucleolar ribonucleoprotein particles. It is therefore likely that any individual protein will be recovered only in very substoichiometric yield in association with Nop1p.

Affinity purification was also performed with ProtA-Nop58ΔKKE. Nop1p was clearly shown to be copurified, but in lower yield (data not shown). The apparent substoichiometric recovery of Nop1p could indicate that only a fraction of the pool of Nop58p is in association with Nop1p but also could simply be due to some dissociation of the complex during purification.

To determine whether all three proteins are present in the same complex, constructs in which the ProtA tags in ProtA-Nop56ΔKKE and ProtA-Nop58ΔKKE were replaced by 3× Myc tags were made. A strain carrying chromosomal deletions of both *NOP56* and *NOP58*, complemented by plasmids expressing ProtA-Nop56ΔKKE and ProtA-Nop58ΔKKE, was constructed. The Myc-tagged constructs were introduced separately into this strain. In both cases, the introduction of the Myc-tagged construct allowed the loss of the plasmid carrying the ProtA-tagged construct with no alteration in growth, showing the Myc-tagged constructs to be functional. These strains were used in an affinity purification experiment (see Materials and Methods). Western blot filters prepared from the eluates were probed with anti-ProtA, anti-Nop1, and anti-Myc antibodies (9E10). Immunoprecipitation of ProtA-Nop56ΔKKE led to the copurification of Myc-Nop58ΔKKE together with Nop1p (Fig. 4B). However, the parallel experiment in which ProtA-Nop58ΔKKE was immunoprecipitated did not result in detectable coprecipitation of Myc-Nop56ΔKKE, although Nop1p was clearly present in the eluate. These results indicate that all three proteins are probably present in a single complex (see also Discussion).

Generation and characterization of thermosensitive alleles of *NOP56*. To analyze the function of Nop56p, mutant alleles were generated in a well-conserved region of the protein and introduced into a *nop56* null strain by plasmid exchange (see Materials and Methods). The effects on growth of two ts alleles identified by screening of the resulting strains are shown in Fig. 5. Strains carrying *nop56-1* exhibit a reduced growth rate at all temperatures. Strains carrying *nop56-2* have a growth rate similar to that of *NOP56*$^+$ cells at 23 and 30°C; following transfer to 37°C, growth slows after 6 to 8 h and cells do not divide after 20 h (Fig. 5A).

The *nop56-1* and *nop56-2* alleles were recovered and sequenced. The mutagenized alleles were also recovered from other strains: two that allowed growth at all temperatures and one allele that was nonfunctional at all temperatures, as shown by the inability of the plasmid exchange strain to grow on medium containing 5-FOA (which selects against the *URA3* marker present on the plasmid that also carries the wild-type *NOP56* gene). The sequences of the mutant alleles were analyzed; *nop56-1* contains two mutations leading to the substitution of Val-333 with Ala and Met-385 with Arg. The single mutation found in *nop56-2* replaced Tyr-355 with Cys. To confirm that this change was responsible for the growth defect of *nop56-2* strains at a restrictive temperature, the 0.5-kb *Nco*I fragment of *NOP56*, which includes the *nop56-2* mutation but has no other changes, was used to replace the corresponding

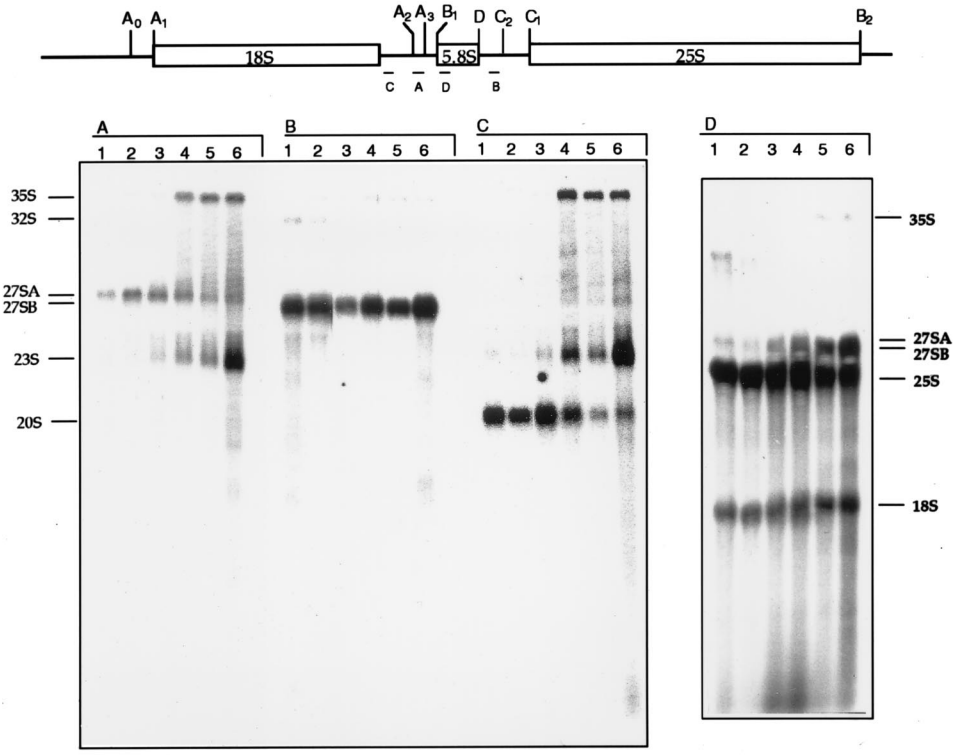

FIG. 7. Steady-state levels of the pre-rRNAs visualized by Northern blot hybridization. For each panel (A to D), lanes 1 and 2 correspond to total RNA extracted from a wild-type strain after growth for 24 h at 23 or 37°C, respectively, and lanes 3 to 6 correspond to total RNA extracted from a *nop56-2* strain (lane 3, 24 h at 23°C; lane 4, 6 h at 37°C; lane 5, 18 h at 37°C; lane 6, 24 h at 37°C). The positions of probes A to D, which were used for panels A to D, respectively, are shown on a diagram of the 35S pre-rRNA. Probe D, which is directed against the mature 5.8S rRNA, cross-hybridizes with mature 18S and 25S rRNA.

fragment in a plasmid carrying the wild-type gene *NOP56*. The resulting plasmid was transformed into the plasmid exchange test strain and gave rise to a ts phenotype.

Function of Nop56p during ribosome biogenesis. As an initial test for detects in ribosome synthesis, the ribosomal protein profile was analyzed by sucrose gradient centrifugation. After incubation of *NOP56* and *nop56-2* strains at 37°C for either 2 or 6 h, proteins were pulse-labeled with [^{35}S]methionine. Cell lysates were fractionated on a 10 to 40% sucrose gradient, and the recovered fractions were analyzed by SDS-PAGE. In the *nop56-2* strain, the peak of 40S subunit proteins matched that in the *NOP56* strain, but no clear peak of 60S proteins was observed in the mutant (data not shown).

To determine whether the apparent deficiency in 60S subunit synthesis in *nop56-2* strains was due to defects in pre-rRNA processing, this was analyzed by pulse-chase labeling (Fig. 6) and Northern blot hybridization (Fig. 7). Following transfer to the nonpermissive temperature for 6 h, the *nop56-2* strain showed lower incorporation of [^{3}H]uracil compared to the *NOP56*$^{+}$ strain; in Fig. 6, the *nop56-2* panel was exposed three times longer than the *NOP56*$^{+}$ panel. Figure 6 reveals a substantial delay in rRNA maturation in the *nop56-2* strain. Mature 25S and 18S rRNA were visible in wild-type cells after 4 min of chase. In contrast, mature 18S rRNA did not clearly accumulate in the *nop56-2* strain until 15 min of chase, while mature 25S was still scarcely detected at this time point. Processing of the 35S pre-rRNA primary transcript is strongly inhibited; a substantial level of 35S remains after a 15-min chase, whereas it is not detected later than 4 min of chase in the wild-type cells, consistent with the time of transcription of the pre-rRNA during which labeled 35S continues to be produced. The normal products of cleavage at sites A_1 and A_2, the 32S 27SA_2, and 20S pre-rRNAs, are strongly reduced (see Fig. 7 for the positions of the cleavage sites). In contrast, the 23S RNA, which is the product of direct cleavage of the 35S pre-rRNA at site A_3 in the absence of upstream processing, is detected in the mutant. The 27SB pre-rRNA is detected in the mutant, but its appearance is strongly delayed.

The steady-state levels of the pre-rRNAs were further examined by Northern blot hybridization (Fig. 7). Following growth at the permissive temperature, no aberrant processing was observed in the *nop56-2* strain (Fig. 7, lanes 3), and all rRNA intermediates exhibited a level similar to that of the wild-type control strain incubated under the same conditions (Fig. 7, lanes 1). Following transfer of the *nop56-2* strain to 37°C, all probes reveal a strong accumulation of the 35S pre-rRNA (Fig. 7, lanes 4 to 6), consistent with the results of pulse-chase labeling. This is associated with the appearance of the 23S pre-rRNA and loss of the 32S, 27SA_2, and 20S pre-rRNAs. Together, these data indicate that processing of the 35S pre-rRNA is strongly inhibited at sites A_0, A_1, and A_2. Some accumulation of the 27SB pre-rRNA is also seen in the *nop56-2* strain, indicating that production of the mature 25S rRNA is also delayed at this processing step. The steady-state level of the mature 18S rRNAs was not clearly reduced in the *nop56-2* strain, and the level of the 25S rRNA was only mildly reduced (Fig. 7D).

We conclude that many pre-rRNA processing steps are inhibited or strongly delayed in the *nop56-2* mutant strain, greatly delaying the synthesis of the mature rRNAs. However, the steady-state levels of the mature rRNAs indicate that their synthesis does continue, and the pre-rRNA processing defect is

therefore unlikely to be the direct cause of lethality in the *nop56-2* mutant strain.

DISCUSSION

sl interactions have recently proved useful for the analysis of large macromolecular structures such as the nuclear pore complex (7, 10) or complex RNA biogenesis pathways such as tRNA processing (42, 43). sl analyses starting with the pre-rRNA processing component have been used to identify three nucleolar proteins, Nop77p (5), Rrp5p (52), and Rok1p (50). Here we report the use of this approach to characterize new components interacting with Nop1p. *NOP56* was identified as sl with *nop1-5*, a ts lethal allele that blocks processing of the pre-RNA. A database search identified Nop58p, which is 45% identical to Nop56p, and a human homolog, hNop56p, that is 52% identical. Expression of the human cDNA in yeast failed to complement a *nop56* null mutation. Subsequently, Nop58p was identified in a screen for mutations that are sl with the *nop1-3* allele that inhibits 2′-O methylation of the pre-rRNA (49). Both Nop56p and Nop58p are essential nucleolar proteins.

Another gene, *NOP77*/*NOP4*, was previously identified as sl with *nop1-5* (5, 46). Comparison of the genomic *NOP77*/*NOP4* allele from the sl mutant with the allele present on the plasmid which suppressed the sl phenotype revealed a single nucleotide change (5). Surprisingly, an independently isolated wild-type clone of *NOP77*/*NOP4* had the same sequence as the gene isolated from the sl mutant (46), indicating that the heterogeneity in the *NOP77*/*NOP4* sequences represented a natural allelic variation between yeast strains.

To assess the role of Nop56p in rRNA processing and ribosome biogenesis, ts mutants were generated. One mutant, *nop56-2*, was chosen for further characterization on the basis of its severely ts phenotype at 37°C. Analysis of this mutant indicated that the phenotype was caused by one mutation (Y355→C) in a region of the protein that is conserved throughout evolution. The pre-rRNA processing defects observed at the restrictive temperature show similarities to those observed for *nop1-5* mutant strains; processing at several sites was inhibited, leading to a delay in the appearance of both 18S and 25S rRNA, with a greater effect on 25S than on 18S processing. The processing defect does not, however, appear to be the direct cause of lethality, since growth inhibition was not accompanied by a strong reduction in the levels of the mature rRNAs. We predict that the primary defect in *nop56-2* strains is in the assembly of the preribosomal particles and/or the folding of the pre-rRNA. The observed delay in pre-rRNA processing may be a consequence of the abnormal structure of the preribosomes in the mutant.

Mutations in Nop77p/Nop4p also inhibit the synthesis of 25S and 5.8S rRNAs, although the phenotype is distinct from that of *nop56-2*, being largely due to the loss of the $27SA_3$ pre-rRNA (5, 46). As with Nop56p, the defect in Nop77p/Nop4p mutant strains was attributed to a primary defect in ribosome assembly, with a secondary defect in pre-rRNA processing (5, 46). Mutations that inhibit pre-rRNA processing have been identified in at least 16 genes that are not predicted to encode actual RNA processing components. These include six predicted RNA helicases and a number of ribosomal proteins, and many or all of these are likely to be required for correct assembly of the preribosomal particles. Why do these mutations inhibit processing? It is possible that the processing nucleases require the correct assembly of a very complex substrate for cleavage. However, the two known endonucleases, RNase MRP and RNase III, can recognize their cleavage sites in the naked pre-rRNA in vitro (8, 26), so this seems unlikely. We believe that in the absence of correct assembly, processing is inhibited by some quality control system (22). In the normal cell, the function of this system would be to delay processing long enough for a missing protein to bind or for some stem to fold correctly, etc.

A striking feature of Nop56p and Nop58p is the presence of KKE/D repeats present at the COOH terminus. Similar repeat sequences are found in the human microtubule-associated proteins MAP1A and MAP1B (23, 35), and KKE/D repeats have been reported to confer microtubule binding activity (37). Highly homologous repeats are present in two other yeast nucleolar proteins; Cbf5p is the putative rRNA pseudouridine synthase and is also required for pre-rRNA processing at sites A_0, A_1, and A_2 (18, 21), while Dbp3p is a putative RNA helicase that is required for normal cleavage at site A_3 (54). The KKE/D motif is not found in any other predicted ORF in the yeast genomic sequence, and its occurrence in four nucleolar proteins would appear to be significant.

Simultaneous deletion of the KKE/D repeats from both Nop56p and Nop58p did not clearly affect cell growth and did not impair the localization of either protein. The motif is therefore not a necessary signal for nuclear or nucleolar localization. The KKE/D domains of Cbf5p and Dbp3p have also been reported to be dispensable (54). Curiously, rat Nap57p, the homolog of Cbf5p (29), and human hNop56p both lack the KKE/D repeat sequences, despite otherwise showing very high conservation. A major difference between yeasts and higher eukaryotes is the closed mitosis in yeasts (i.e., the nuclear membrane remains intact during cell division in yeasts). This means that all of the nuclear contents, including the nucleolus and the ribosome synthesis machinery, must be segregated to the daughter nuclei. We speculate that the KKE/D domains do indeed confer microtubule binding activity. This may aid the efficient and accurate segregation of the pre-rRNA processing machinery during mitosis. In the absence of the KKE/D repeats, segregation of the nucleolar components would be somewhat less accurate, but this might not affect growth under most conditions. Alternatively, the presence of a KKE/D repeat on only one protein might be sufficient to support normal cell growth. In the case of the RNA binding motif present in nucleoporins Nup145p, Nup116p, and Nup100p, deletion of the motif from all three proteins was needed for lethality (10).

Nop56p is recovered from cell lysates in a stoichiometric complex with Nop1p. Moreover, Nop58p could also be coprecipitated with Nop56p, indicating that a trimeric Nop56p-Nop58p-Nop1p complex exists. Nop58p is also associated with Nop1p, but recovery of Nop1p with Nop58p is substoichiometric. This might, however, be due to partial dissociation during purification of the ProtA-Nop58p complex. We can exclude nonspecific interactions due to the KKE/D motifs, since Nop1p was recovered in association with both Nop56p and Nop58p when tagged constructions lacking the KKE/D motif were used, and no coprecipitation was observed when a nonfunctional version of Nop56p was used for affinity purification (data not shown). No protein of the size of Nop77p/Nop4p was detected in the Nop56p precipitate, and Nop77p coprecipitates only a small amount of Nop1p (5), showing that it cannot be a stable component of the Nop56p-Nop1p complex. No snoRNAs were detectably coprecipitated with the Nop1p-Nop56p complex, and the phenotypes of the *nop1-5* and *nop56-2* mutations do not resemble those seen on mutation of any characterized snoRNA. We conclude that the function of the Nop1p-Nop56p complex in ribosome synthesis is probably not mediated by snoRNAs.

Despite the homology between Nop56p and Nop58p,

NOP58 cannot complement the *nop1-5* sl strain and *NOP56* cannot complement the *nop1-3* sl strain. We predict that the point mutations in *nop1-5* and *nop1-3* specifically interfere with the normal interaction of Nop1p with Nop56p and Nop58p, respectively. These would be sl in combination with mutations in Nop56p and Nop58p which interfere with normal binding to Nop1p. The phenotype of the *nop56-2* mutation resembles that of *nop1-5*; it will be of interest to determine whether the phenotype of a conditional *nop58* allele resembles that of *nop1-3*.

In conclusion, we believe that a complex between Nop1p and Nop56p is required for a step(s) in ribosome assembly that does not involve the snoRNAs. Nop77p is not a stable component of the complex but functionally interacts with it. Given the high evolutionary conservation, we would predict that fibrillarin and hNop56p have a similar function in human cells.

ACKNOWLEDGMENTS

We thank the members of the Tollervey laboratory for helpful discussion and valuable assistance in the rRNA processing analysis and John Aris for the gift of A66 antibodies. The critical reading of the manuscript by the members of the laboratory is gratefully acknowledged.

T.G. was the recipient of a Human Frontier Scientific Program fellowship (LT473/94), and E.H. was the recipient of a grant from the DFG (Hu363/4-3).

REFERENCES

1. **Aris, J. P., and G. Blobel.** 1991. cDNA cloning and sequencing of human fibrillarin, a conserved nucleolar protein recognized by autoimmune antisera. Proc. Natl. Acad. Sci. USA **88:**931–935.
2. **Bachellerie, J. P., B. Michot, M. Nicoloso, A. G. Balakin, J. Ni, and M. Fournier.** 1995. Antisense snoRNAs: a family of nucleolar RNAs with long complementarities to rRNA. Trends Biochem. Sci. **20:**261–264.
3. **Balakin, A. G., L. Smith, and M. J. Fournier.** 1996. The RNA world of the nucleolus: two major families of small RNAs defined by different box elements with related functions. Cell **86:**823–834.
4. **Beltrame, M., and D. Tollervey.** 1995. Base-pairing between U3 and the pre-ribosomal RNA is required for 18S rRNA synthesis. EMBO J. **14:**4350–4356.
5. **Bergès, T., E. Petfalski, D. Tollervey, and E. C. Hurt.** 1994. Synthetic lethality with fibrillarin identifies NOP77p, a nucleolar protein required for pre-rRNA processing and modification. EMBO J. **13:**3136–3148.
6. **Bousquet-Antonelli, C., Y. Henry, J.-P. Gèlugne, M. Caizergues-Ferrer, and T. Kiss.** 1997. A small nucleolar RNP protein is required for pseudouridylation of eukaryotic ribosomal RNAs. EMBO J. **16:**4770–4776.
7. **Doye, V., and E. C. Hurt.** 1995. Genetic approaches to nuclear pore structure and function. Trends Genet. **11:**235–241.
8. **Elela, S. A., H. Igel, and M. Ares, Jr.** 1996. RNase III cleaves eukaryotic preribosomal RNA at a U3 snoRNP-dependent site. Cell **85:**115–124.
9. **Elledge, S. J., and R. W. Davis.** 1988. A family of versatile centromeric vectors designed for use in the sectoring-shuffle mutagenesis assay in Saccharomyces cerevisiae. Gene **70:**303–312.
10. **Fabre, E., W. C. Boelens, C. Wimmer, I. W. Mattaj, and E. C. Hurt.** 1994. Nup145p is required for nuclear export of mRNA and binds homopolymeric RNA in vitro via a novel conserved motif. Cell **78:**275–289.
11. **Ganot, P., M.-L. Bortolin, and T. Kiss.** 1997. Site-specific pseudouridine formation in preribosomal RNA is guided by small nucleolar RNAs. Cell **89:**799–809.
12. **Ganot, P., M. Caizergues-Ferrer, and T. Kiss.** 1997. The family of box ACA small nucleolar RNAs is defined by an evolutionarily defined secondary structure and ubiquitous sequence elements essential for RNA accumulation. Genes Dev. **11:**941–956.

12a. **Gautier, T.** Unpublished data.

13. **Grandi, P., V. Doye, and E. C. Hurt.** 1993. Purification of NSP1 reveals complex formation with 'GLFG' nucleoporins and a novel nuclear pore protein NIC96. EMBO J. **12:**3061–3071.
14. **Hadjiolov, A. A.** 1985. Cell biology monographs, vol. 12. The nucleolus and the ribosome biogenesis. Springer-Verlag, Vienna, Austria.
15. **Hughes, J. M. X., and M. Ares, Jr.** 1991. Depletion of U3 small nucleolar RNA inhibits cleavage in the 5′ external transcribed spacer of yeast pre-ribosomal RNA and impairs formation of 18S ribosomal RNA. EMBO J. **10:**4231–4239.
16. **Jansen, R. P., E. C. Hurt, H. Kern, H. Lehtonen, M. Carmo-Fonseca, B. Lapeyere, and D. Tollervey.** 1991. Evolutionary conservation of the human protein fibrillarin and its functional expression in yeast. J. Cell Biol. **113:**715–727.
17. **Jansen, R. P., D. Tollervey, and E. C. Hurt.** 1993. A U3 snoRNP protein with homology to splicing factor PRP4 and Gb domains is required for ribosomal RNA processing. EMBO J. **12:**2549–2558.
18. **Jiang, W., K. Middleton, H.-J. Yoon, F. Claire, and C. John.** 1993. An essential yeast protein, CBF5p, binds in vitro to centromeres and microtubules. Mol. Cell. Biol. **13:**4884–4893.
19. **Kiss-Laszlo, Z., Y. Henry, J. Bachellerie, M. Caizergues-Ferrer, and T. Kiss.** 1996. Site-specific ribose methylation of preribosomal RNA: a novel function for small nucleolar RNAs. Cell **85:**1077–1088.
20. **Kranz, J. E., and C. Holm.** 1990. Cloning by function: an alternative approach for identifying yeast homologs of genes from other organisms. Proc. Natl. Acad. Sci. USA **87:**6629–6633.
21. **Lafontaine, D., C. Bousquet-Antonelli, Y. Henry, M. Caizergues-Ferrer, and D. Tollervey.** Submitted for publication.
22. **Lafontaine, D., J. Vanderhaute, and D. Tollervey.** 1995. The 18S rRNA dimethylase Dim1p is required for pre-ribosomal RNA processing in yeast. Genes Dev. **9:**2470–2481.
23. **Langkopf, A., J. A. Hammarback, R. Mueller, R. B. Vallee, and C. C. Garner.** 1992. Microtubule-associated proteins 1A and LC2. J. Biol. Chem. **267:**16561–16566.
24. **Leung, D., E. Chen, and D. Goeddel.** 1989. A method for random mutagenesis of a defined DNA segment using a modified polymerase chain reaction. J. Methods Cell Mol. Biol. **1:**11–15.
25. **Li, H. V., J. Zagorski, and M. J. Fournier.** 1990. Depletion of U14 small nuclear RNA (snR128) disrupts production of 18S rRNA in *Saccharomyces cerevisiae*. Mol. Cell. Biol. **10:**1145–1152.
26. **Lygerou, Z., C. Allmang, D. Tollervey, and B. Séraphin.** 1996. Accurate processing of a eukaryotic precursor ribosomal RNA by ribonuclease MRP in vitro. Science **272:**268–270.
27. **Maden, B. E. H.** 1990. The numerous modified nucleotides in eukaryotic ribosomal RNA. Prog. Nucleic Acid Res. Mol. Biol. **39:**241–303.

27a. **Maniatis, T., E. F. Fritsch, and J. Sambrook.** 1982. Molecular cloning: a laboratory manual. Cold Spring Harbor Laboratory Press, Cold Spring Harbor, N.Y.

28. **Maxwell, E. S., and M. J. Fournier.** 1995. The small nucleolar RNAs. Annu. Rev. Biochem. **35:**897–934.
29. **Meier, U. T., and G. Blobel.** 1994. NAP57, a mammalian nucleolar protein with a putative homolog in yeast and bacteria. J. Cell Biol. **127:**1505–1514.
30. **Mitchell, P., E. Petfalski, and D. Tollervey.** 1996. The 3′ end of yeast 5.8S rRNA is generated by an exonuclease processing mechanism. Genes Dev. **10:**502–513.
31. **Morin, J. P., J. A. Downs, A. M. Snodgrass, and T. D. Gilmore.** 1995. Genetic analysis of growth inhibition by GAL4-IκB-α in *Saccharomyces cerevisiae*. Cell Growth Differ. **6:**789–798.
32. **Morrissey, J., and D. Tollervey.** 1993. Yeast snR30 is a small nucleolar RNA required for 18S rRNA synthesis. Mol. Cell. Biol. **13:**2469–2477.
33. **Ni, J., A. L. Tien, and M. J. Fournier.** 1997. Small nucleolar RNAs direct site-specific synthesis of pseudouridine in ribosomal RNA. Cell **89:**565–573.
34. **Nigg, E. A.** 1988. Nuclear function and organization: the potential of immunochemical approaches. Int. Rev. Cytol. **110:**27–92.
35. **Noble, M., S. A. Lewis, and N. J. Cowan.** 1989. The microtubule binding domain of microtubule-associated protein MAP1B contains a repeated sequence motif unrelated to that of MAP2 and tau. J. Cell Biol. **109:**3367–3376.
36. **Pearson, B. M., Y. Hernando, J. Payne, S. S. Wolf, A. Kalogeropoulos, and M. Schweizer.** 1996. Sequencing of a 35.71 kb DNA segment on the right arm of yeast chromosome XV reveals regions of similarity to chromosomes I and XIII. Yeast **12:**1021–1031.
37. **Pedrotti, B., and K. Islam.** 1994. Purified native microtubule associated protein MAP1A: kinetics of microtubule assembly and MAP1A/tubulin stoichiometry. Biochemistry **33:**12463–12470.
38. **Sanger, F., S. Nicklen, and A. R. Coulson.** 1977. DNA sequencing with chain-terminating inhibitors. Proc. Natl. Acad. Sci. USA **74:**5463–5467.
39. **Scheer, U., and D. Weisenberger.** 1994. The nucleolus. Curr. Opin. Cell Biol. **6:**354–359.
40. **Sherman, F., G. R. Fink, and J. B. N. Hicks.** 1986. Methods in yeast genetics. A laboratory course manual. Cold Spring Harbor Laboratory Press, Cold Spring Harbor, N.Y.
41. **Sikorski, R. S., and P. Hieter.** 1989. A system of shuttle vectors and yeast host strains designed for efficient manipulation of DNA in *Saccharomyces cerevisiae*. Genetics **122:**19–27.
42. **Simos, G., A. Segref, F. Fasiolo, K. Hellmuth, A. Shevchenko, M. Mann, and E. C. Hurt.** 1996. The yeast protein Arc1p binds to tRNA and functions as a cofactor for the methionyl- and glutamyl-tRNA synthetases. EMBO J. **15:**5437–5448.
43. **Simos, G., H. Tekotte, H. Grosjean, A. Segref, K. Sharma, D. Tollervey, and E. C. Hurt.** 1995. Nuclear pore proteins are involved in the biogenesis of functional tRNA. EMBO J. **15:**2270–2284.
44. **Siniossoglou, S., P. Grandi, and E. C. Hurt.** Affinity purification of protein A-tagged nuclear pore proteins from yeast. *In* Cell biology: a laboratory handbook, vol. 2, 2nd ed., in press. Academic Press, New York, N.Y.
45. **Sommerville, J.** 1986. Nucleolar structure and ribosome biogenesis. Trends Biochem. Sci. **11:**438–442.

46. **Sun, C., and J. L. Woolford, Jr.** 1994. The yeast *NOP4* gene product is an essential nucleolar protein required for pre-rRNA processing and accumulation of 60S ribosomal subunits. EMBO J. **13:**3127–3135.
47. **Tollervey, D.** 1987. A yeast small nuclear RNA is required for normal processing of pre-ribosomal RNA. EMBO J. **6:**4169–4175.
48. **Tollervey, D., and T. Kiss.** 1997. Function and synthesis of small nucleolar RNAs. Curr. Opin. Cell Biol. **9:**337–342.
49. **Tollervey, D., H. Lehtonen, R. P. Jansen, H. Kern, and E. C. Hurt.** 1993. Temperature-sensitive mutations demonstrate roles for yeast fibrillarin in pre-rRNA processing, pre-rRNA methylation, and ribosome assembly. Cell **72:**443–457.
50. **Venema, J., C. Bousquet-Antonelli, J.-P. Gelugne, M. Caizergues-Ferrer, and D. Tollervey.** 1997. Rok1p is a putative RNA helicase required for rRNA processing. Mol. Cell. Biol. **17:**3398–3407.
51. **Venema, J., and D. Tollervey.** 1995. Processing of pre-ribosomal RNA in *Saccharomyces cerevisiae*. Yeast **11:**1629–1650.
52. **Venema, J., and D. Tollervey.** 1996. RRP5 is an essential yeast gene required for formation of both 18S and 5.8S rRNA. EMBO J. **15:**5701–5714.
53. **Warner, J. R.** 1990. The nucleolus and ribosome formation. Curr. Opin. Cell Biol. **2:**521–527.
54. **Weaver, P., C. Sun, and T.-H. Chang.** 1997. Dbp3p, a putative RNA helicase in *Saccharomyces cerevisiae*, is required for efficient pre-rRNA processing predominantly at site A_3. Mol. Cell. Biol. **17:**1354–1365.
55. **Weidenhammer, E. M., M. Singh, and J. L. Woolford.** 1996. The PRP31 gene encodes a novel protein required for pre-mRNA splicing in Saccharomyces cerevisiae. Nucleic Acids Res. **24:**1164–1170.